Optimal Design of Permanent Magnetic Actuator for Permanent Magnet Reduction and Dynamic Characteristic Improvement using Response Surface Methodology

Hyun-Mo Ahn*, Tae-Kyung Chung**, Yeon-Ho Oh***, Ki-Dong Song***, Young-Il Kim§, Heung-Ryeol Kho§, Myeong-Seob Choi§ and Sung-Chin Hahn†

Abstract – Permanent magnetic actuators (P.M.A.s) are widely used to drive medium-voltage-class vacuum circuit breakers (V.C.B.s). In this paper, a method for design optimization of a P.M.A. for V.C.B.s is discussed. An optimal design process employing the response surface method (R.S.M.) is proposed. In order to calculate electromagnetic and mechanical dynamic characteristics, an initial P.M.A. model is subjected to numerical analysis using finite element analysis (F.E.A.), which is validated by comparing the calculated dynamic characteristics of the initial P.M.A. model with no-load test results. Using tables of mixed orthogonal arrays and the R.S.M., the initial P.M.A. model is optimized to minimize the weight of the permanent magnet (P.M.) and to improve the dynamic characteristics. Finally, the dynamic characteristics of the optimally designed P.M.A. are compared to those of the initially designed P.M.A.

Keywords: Permanent magnetic actuators, Finite element analysis, Optimization methods, Permanent magnetic machines, Response surface method

1. Introduction

In recent years, the growing prospect of the electric power industry in a green and eco-friendly manner has gained much attention. Vacuum circuit breakers (V.C.B.s), which use vacuum as an insulation medium, are replacing gas circuit breakers (G.C.B.s) for use in medium-voltage-class power interception [1-3].

Switch actuators for V.C.B.s typically use spring, solenoid, or permanent magnetic actuator (P.M.A.) mechanisms, and medium-voltage-class V.C.B.s have been using spring-driven mechanism for decades. Such mechanisms, however, have drawbacks including complicated structures, reliance on periodic maintenance, and proneness to oil leaks. P.M.A.s, by contrast, have advantages in terms of simpler structure, improved operating time, easy motion control, and high reliability. Accordingly, manufacturers seeking to reduce the V.C.B. size and to improve the operating time have begun to prefer P.M.A. over spring-driven mechanism [4, 5].

Fig. 1 shows the structure of the P.M.A. developed for use in a V.C.B. It has four important electromechanical components: the permanent magnets (P.M.s), a movable plunger, trip coils, and static yokes. When an excitation current is supplied through the trip coil, the plunger moves upwards or downwards. The mechanical energy generated due to movement of plunger is transmitted to a vacuum interrupter (V.I.). When the plunger reaches fully open or closed position, it stops to be held still by P.M.s only. The P.M.s, which together with the trip coil compose the P.M.A., are able to generate rapid continuous motion with more efficiency than a spring-type actuator [6-8].

The response surface method (R.S.M.) is an effective statistical technique that can be used to improve the performance of electrical devices, enabling the easy development of objective functions and the reduction of computing time [9, 10].
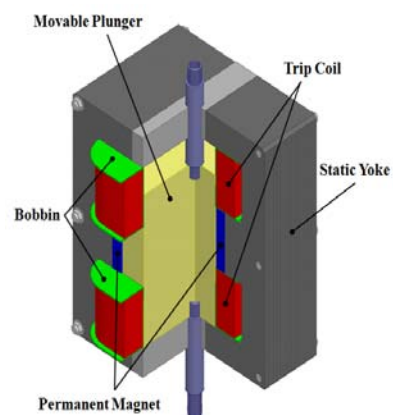
† Corresponding Author: Dept. of Electrical Engineering, Dong-A University, Korea. (schahn@dau.ac.kr)
* Dept. of Electrical Engineering, Dong-A University, Korea. (hmahn @donga.ac.kr)
** School of Electrical and Electronics Engineering, Chung-Ang University, Korea. (tkchung@cau.ac.kr)
*** Power Apparatus Research Center, HVDC Research Division, Korea Electrotechnology Research Institute, Korea. (yhoh@keri.re.kr)
§ ENTEC Electric & Electronic Co., Ltd., Korea. (hrkoh@entecene. co.kr)

Fig. 1. Structure of P.M.A. model

935

As most types of electric machines have many design parameters, it is often necessary to search extensively in order to determine which particular variable most affects relevant design results. Because the R.S.M. is generally used to optimize two or three design variables [11], design of experiments (D.O.E.s) for seven design variables can be developed using tables of mixed orthogonal arrays to assess large numbers of design variables and their levels effectively [12], with a response value for each parameter combination calculated by means of finite element analysis (F.E.A.). Using the R.S.M., the D.O.E.s according to tables of mixed orthogonal arrays are analyzed. A Pareto chart can be used in order to find the design variables with the largest effects on the response function [13]. The P.M.A. design optimization process proposed here is aimed at minimizing the weight of the P.M. at improving the dynamic characteristics of an initially designed P.M.A.

This paper describes a dynamic characteristic analysis of a P.M.A. using coupled finite element method (F.E.M.) and the design optimization of the P.M.A. using tables of mixed orthogonal arrays and the R.S.M. Using coupled F.E.M., electromagnetic and mechanical characteristics such as the holding force and the action complete time are calculated and used as response values for P.M.A. design optimization. In order to verify the validity of the F.E.A., the calculated dynamic characteristics of an initial P.M.A. model are compared with no-load test results. Finally, the optimal P.M.A. model designed by using the R.S.M. is compared with the initial P.M.A. model in order to verify the validity of the optimally designed model.

2. Characteristic of V.C.B. Mechanism

The force characteristics of the actuators used for driving a vacuum interrupter (V.I.) are shown in Fig. 2 [6, 14]. It can be seen that 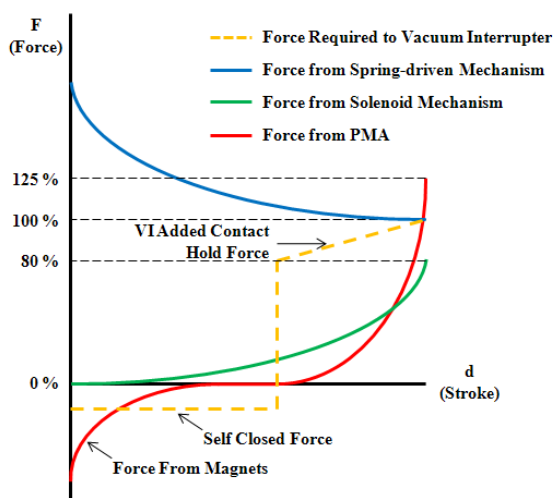the V.I. requires a high level of thrust at the end of stroke. Although the spring actuator produces high levels of thrust in the initial operation, this drops by the end of the stroke; in addition, spring actuators have complicated structures and face limitations to continuous operation. Although the solenoid actuator generates a similar force profile as that required by the V.I., this doesn't reach the required force of V.I. at the end of the stroke [15]. By contrast, the P.M.A. matches the force characteristics of the V.I. closely during the initial operation of the stroke and also produces high levels of thrust at the end of the stroke, making it a more efficient V.I. driver than either the spring actuator or the solenoid.

3. Numerical Analysis Model

As shown in Fig. 3, the P.M.A. model used in this study consists of trip coils, plunger, yokes, and P.M.s, which are placed in the center of the P.M.A. between the yoke and the plunger. The holding force generated by the P.M.s maintains the position of the plunger. At that time, when an excitation current flows in the upper or lower coil, the P.M.A. performs an open or close operation. The nonlinear B-H characteristic of plunger and yoke is shown in Fig. 4.
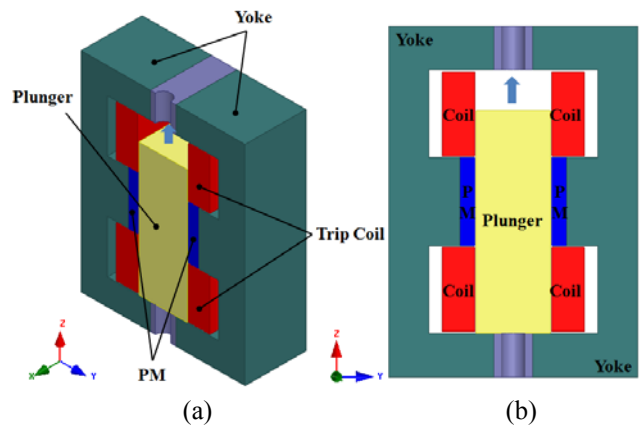

(a)   (b)
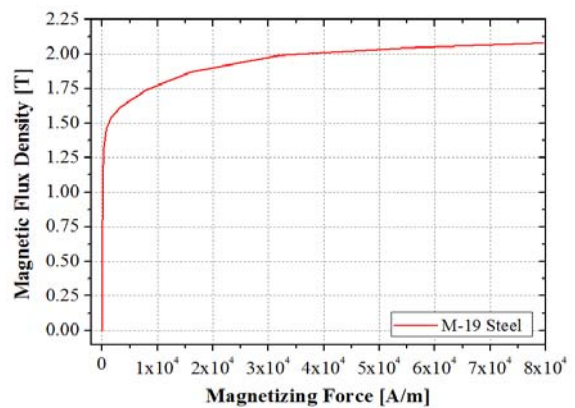
Fig. 3. P.M.A. Model (a) side-view (b) front-view

Fig. 4. B-H curve of M-19 steel

Fig. 2. Force characteristic of V.C.B. mechanism

4. Numerical Analysis and Experimental Validation

Generally, a P.M.A. can be adequately represented in a mathematical manner through the following three equations: (a) the electric circuit equation with voltage source, (b) the magnetic field equation for magnetic flux and energy, and (c) the equation of motion for velocity and force [5, 8, 16].

4.1 Governing equation

To analyze the dynamic characteristics of the P.M.A. model, the electric circuit equation should be coupled to the magnetic field equation. When a source voltage is charged to the capacitor for the driving source, the electric circuit equation can be expressed as

$$\frac{1}{C}\int i(t)dt = R \cdot i(t) + \frac{d\lambda}{dt} = R \cdot i(t) + L\frac{di(t)}{dt} \qquad (1)$$

where, C is the capacitance of capacitor for the driving source [F], $i(t)$ is the excitation current [A], R is the resistance [Ω], and L is the inductance [H]. The current density generated by the source capacitor and the P.M. are fundamental to determining the dynamics of the drive plunger, and the magnetic field equation for the P.M.A. is formulated as

$$\nabla \times \nu(\nabla \times \vec{A}) + \sigma\left(\frac{\partial \vec{A}}{\partial t} + \nabla V\right) = \vec{J} + \frac{1}{\mu}(\nabla \times \vec{M}) \qquad (2)$$

where ν is the magnetic reluctivity, $\vec{A}$ is the magnetic vector potential, σ is the conductivity [S/m], $\vec{J}$ is the current density [A/m²], V is the electric potential, μ is the permeability, and $\vec{M}$ is the magnetization vector [A/m]. In terms of the P.M.A. model, the most important parameter from the magnetic field equation above is the magnetic energy, which operates the plunger. The magnetic force can be calculated using the principle of virtual work and is given by

$$F_{mag} = \frac{\partial}{\partial z}\left(\int_{v}\frac{B^2}{2\mu_0}dv\right) \qquad (3)$$

where F_{mag} is the magnetic force [N], z is the motional direction [m], and v is the volume [m³]. This calculated magnetic force is used to build an equation of motion from which plunger acceleration, velocity, and position can be extracted; this is expressed as

$$F_{mag} = M\frac{d^2z}{dt^2} + B\frac{dz}{dt} + K \cdot z + f \qquad (4)$$

where M is the plunger mass [kg], (d^2z/dt^2) is its acceleration in the direction of motion [m/s²], B is the attenuation constant [N/m/s], (dz/dt) is the plunger velocity in the direction of motion [m/s], K is the spring constant [N/m], and f is the frictional force [N].

4.2 Comparison of simulation and experiment

In order to determine the holding force, it is necessary to understand the distribution of magnetic flux density in the absence of excitation current. Using F.E.M., the magnetic flux density distribution can be numerically calculated, as shown in Fig. 5. In this figure, most of the magnetic flux flow occurs on the lower part of the P.M.A. model because the upper part has relatively high magnetic reluctance due to the air gap between the plunger and the upper yoke. With the plunger in the position show, the holding force calculated by F.E.A. is 7777.2 [N], which agrees closely with the value obtained from no-load test.

In order to accurately analyze the dynamic characteristics of the P.M.A., an understanding of the electromagnetic field-circuit link is necessary. To analyze this, an external electric circuit was coupled to the electromagnetic-circuit equation, as show in Fig. 6.

As seen in Fig. 7, the excitation current calculated from simulation is compared with experimental value of no-load test from t=0 to t=70 [ms] and the maximum excitation current calculated by simulation is 107.3 [A], which represents a pattern similar to the current wave obtained from the no-load test. Dynamic characteristic of the plunger was calculated using a coupled electromagnetic-
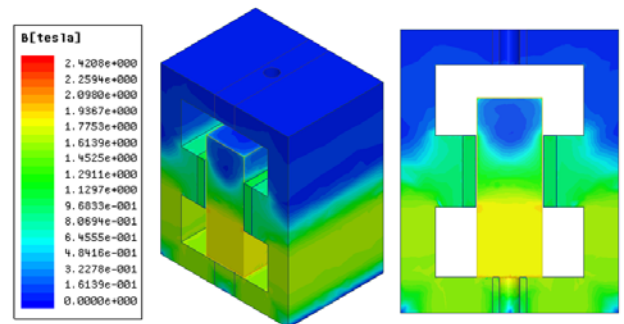
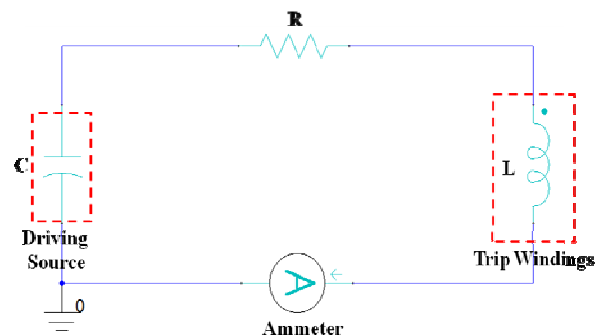**Fig. 5.** Magnetic flux density at no-load condition
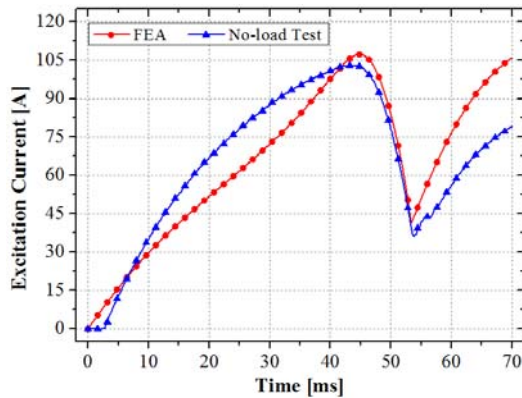
Fig. 6. Drive system

Fig. 7. Comparison of excitation current of simulation and no-load test
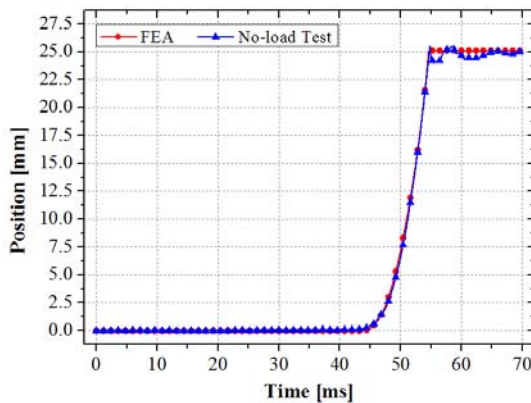

Fig. 8. Comparison of operating time of simulation and no-load test

Table 1. Dynamic characteristics of initial P.M.A. model

Classification	F.E.A.	No-load Test	Error
Holding Force	7777.2 [N]	7710 [N]	0.9 [%]
Peak Current	107.3 [A]	102.9 [A]	4.3 [%]
Action Complete Time	54.8 [ms]	54.8 [ms]	0 [%]

mechanical F.E.A. Fig. 8 shows a comparison of the operating time between the experimental and the F.E.A. values. The plunger action complete time calculated by F.E.A. is 54.8 [ms], which shows good agreement with the experimental value obtained from no-load test.

The dynamic characteristics of initial P.M.A. by F.E.A. are compared with the experimental results measured from no-load test and are shown in Table 1. This table summarizes the close agreement of results discussed above. The P.M.A. design optimization described in this paper is performed based on the results of F.E.A.

5. Design Optimization

5.1 Response surface method [17]

R.S.M., an effective statistical technique for improving electrical device performance, is used for design optimization of the P.M.A. model. R.S.M. uses a statistical method to develop an approximate response formula expressing the correlation between the design variables and the response variables [10]. Schematically, the response η to k design variables can be expressed as

$$\eta = F(x_1, x_2, \cdots, x_k) \tag{5}$$

If a secondary regression model is used for function approximation, this equation can be re-formulated as follows [10, 18, 19]:

$$y = \beta_0 + \sum_{j=1}^{k} \beta_j x_j + \sum_{j=1}^{k} \beta_{jj} x_j^2 + \sum_{i \neq j}^{k} \beta_{ij} x_i x_j + \varepsilon \tag{6}$$

where, β represents the regression coefficients, the indexed x variables are the design variables, ε is the random error, and k is the number of design variables. The least-squares method (L.S.M.) can be used to predict the unknown coefficients. In matrix notation of the fitted coefficients and response model can be expressed as follows [11]:

$$\hat{\beta} = (X'X)^{-1} X'u \quad \hat{u} = X\hat{\beta} \tag{7}$$

where, $\hat{\beta}$ is the vector containing the unknown coefficients. To optimize the design of initial P.M.A. model, we propose the optimal design process shown in Fig. 9.
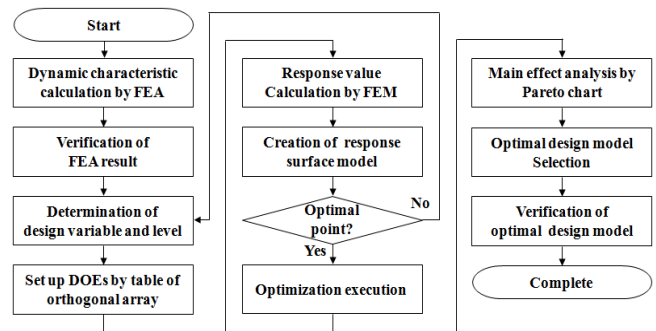

Fig. 9. Design optimization process

5.2 Design variables and levels

In R.S.M., the selection of design variables is very important [9]; however, as most electric machines have a large number of design parameter, D.O.E.s of seven design variables made by using tables of mixed orthogonal arrays is used in order to perform an effective analysis in this study. The seven dimensions selected as design variables are shown in Fig. 10. The design variables have three levels, and these are all shown in Table 2 in which second level of design variables contains values from initial P.M.A. model.
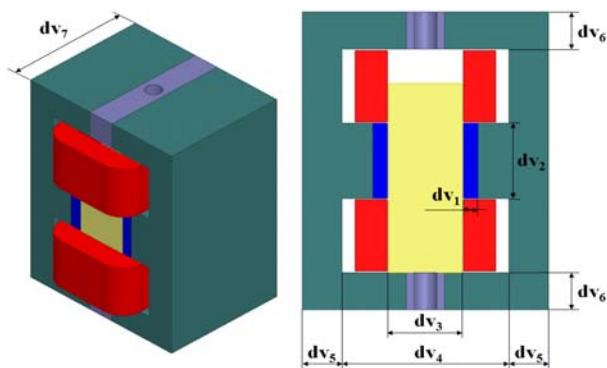
Fig. 10. P.M.A. design variables

Table 2. Design variables and levels

Levels	Design Variables						
	dv_1	dv_2	dv_3	dv_4	dv_5	dv_6	dv_7
1(-1)	8	49.2	47	104	24	24	115
2 (0)	10	54.2	50	114	27	27	125
3 (1)	12	59.2	53	124	30	30	135

5.3 Optimal design result

The mixed orthogonal arrays of D.O.E.s shown in Table 3, which represent design variables considered at each level and response values obtained from F.E.A., are used to perform an R.S.M. design optimization of the P.M.A. model. The response functions are the holding force, maximum thrust, action complete time, and P.M. weight, and the response values for each parameter combination are calculated by F.E.A.

In order to visualize the impact of each design variable on the response function, the main effects of each function are represented with the analysis of variance (A.N.O.V.A.), as shown in Fig. 11.

It can be seen that the holding force and the max thrust are maximized at dv_3 (1), dv_5 (1), and dv_7 (1). Conversely, the action complete time is minimized at dv_3 (1), dv_5 (1), and dv_7 (1). The P.M. weight is minimized at dv_1 (-1), dv_2 (-1), and dv_7 (-1).

In order to draw a response surface based on the

Table 3. Table of mixed orthogonal array $L_{36}(2_1 \times 3_7)$

No.	Design Variables							Holding force [N]	Max thrust force [N]	Action complete time [ms]	P.M.weight [g]
	DV_1	DV_2	DV_3	DV_4	DV_5	DV_6	DV_7				
1	8	49.2	47	104	24	24	115	6152.2	10053.4	65.2	335
2	10	54.2	50	114	27	27	125	7777.2	11173.2	54.8	501.4
3	12	59.2	53	124	30	30	135	9486.8	11988.6	54.2	709.7
4	8	49.2	47	104	27	27	125	7226.6	10963	55.8	364.1
5	10	54.2	50	114	30	30	135	8860.8	11768.8	54	541.5
6	12	59.2	53	124	24	24	115	6677.9	10196.9	57.5	604.6
7	8	49.2	50	124	24	27	135	7369.8	11580.5	55	393.2
8	10	54.2	53	104	27	30	115	7287.3	10989.9	55	461.2
9	12	59.2	47	114	30	24	125	7899.7	10676.2	57.2	657.1
10	8	49.2	53	114	24	30	125	6744.7	11436.2	55.5	364.1
11	10	54.2	47	124	27	24	135	8006.5	11146.9	55	541.5
12	12	59.2	50	104	30	27	115	7743.8	10657.6	56.4	604.6
13	8	54.2	53	104	30	27	115	7156.3	10849.5	55	369
14	10	59.2	47	114	24	30	125	7696.3	10967.5	59.6	547.6
15	12	49.2	50	124	27	24	135	7792.9	11252.9	54.4	589.8
16	8	54.2	53	114	24	24	135	7194.1	11176.2	55	433.2
17	10	59.2	47	124	27	27	115	7310.5	10335.7	64.2	503.8
18	12	49.2	50	104	30	30	125	7980.5	11338.3	54.4	546.1
19	8	54.2	47	124	30	30	115	7136.1	10566.1	58.8	369
20	10	59.2	50	104	24	24	125	7261.9	10676.5	56.8	547.6
21	12	49.2	53	114	27	27	135	8122	11755.6	54.4	589.8
22	8	54.2	50	124	30	24	125	7244.9	10782.3	55	401.1
23	10	59.2	53	104	24	27	135	8030	11648.6	54.8	591.4
24	12	49.2	47	114	27	30	115	7092.3	10538.4	59.8	502.4
25	8	59.2	50	104	27	30	135	8596.8	11755.1	54.8	473.1
26	10	49.2	53	114	30	24	115	6517.4	10326.2	56.2	418.7
27	12	54.2	47	124	24	27	125	7570.9	10863.1	57.2	601.6
28	8	59.2	50	114	27	24	115	6811.2	10210.3	58.4	403
29	10	49.2	53	124	30	27	125	7578.3	11351.3	54.6	455.1
30	12	54.2	47	104	24	30	135	8228.2	11436.6	55.2	649.7
31	8	59.2	53	124	27	30	125	7994.4	11470.7	54.4	438.1
32	10	49.2	47	104	30	24	135	7810.8	11196.1	54.6	491.5
33	12	54.2	50	114	24	27	115	6927.5	10545.4	59.2	553.5
34	8	59.2	47	114	30	27	135	8474.6	11495	55.8	473.1
35	10	49.2	50	124	24	30	115	6557.8	10718	59.2	418.7
36	12	54.2	53	104	27	24	125	7437.5	10736.5	54	601.6

experimental data from Table 3, the response function is extracted by the R.S.M. in accordance with the aim of this study to minimize the weight of the P.M. and to improve the dynamic characteristics of an initially designed P.M.A. In other words, the proposed P.M.A. optimal design process attempts to improve the action complete time (y_T) while minimizing PM weight (y_W) maintaining the holding force (y_{HF}) and maximum thrust (y_{TF}). The two fitted
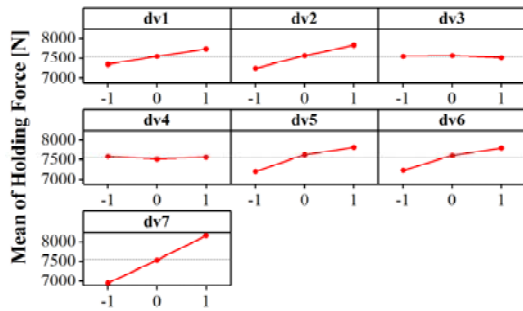

(a)

(b)

(c)

(d)

Fig. 11. Main effect analysis for (a) holding force; (b) max thrust force; (c) complete time; (d) P.M. weight

second-order polynomial response functions of seven design variables that result from this can be expressed as

$$y_{HF} = 12729.8 + 146dv_1 + 222.2dv_2 - 531.3dv_3$$
$$- 35.6dv_4 - 365.2dv_5 + 211.2dv_6 - 45.6dv_7 \quad (8)$$
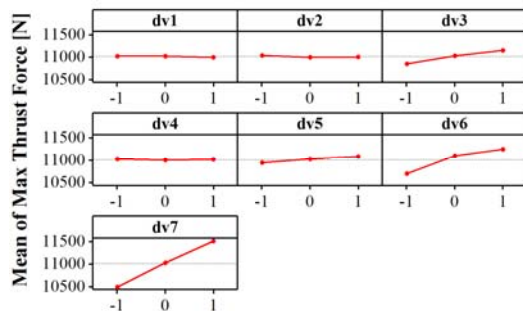$$- 10.6dv_1^2 - 10dv_6^2 + 15dv_3dv_5$$

$$y_{TF} = -10999.5 - 401.1dv_1 + 249.1dv_2 + 116.9dv_3$$
$$- 83.3dv_4 + 1031.3dv_5 + 309.2dv_6 - 74.4dv_7 \quad (9)$$
$$- 14.2dv_6^2 + 10.1dv_3dv_6$$

$$y_T = 1429.6 + 25.5dv_1 + 0.4dv_2 - 20.5dv_3 - 5.5dv_4$$
$$- 48.4dv_5 + 22.7dv_6 - 5dv_7 - 0.5dv_1^2 + 0.4dv_5^2$$
$$- 0.3dv_1dv_2 + 0.1dv_1dv_3 + 0.3dv_1dv_5 - 0.4dv_1dv_6 \quad (10)$$
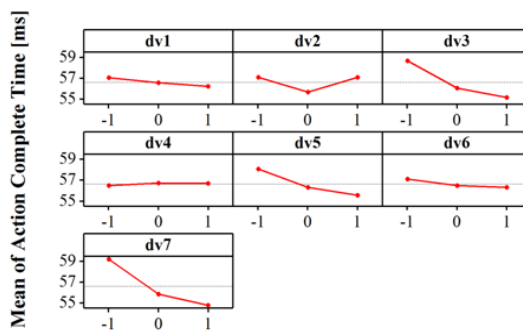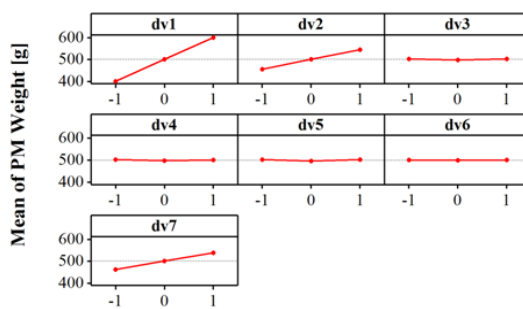$$+ 0.1dv_2dv_5 + 0.3dv_3dv_5 - 0.2dv_5dv_6$$

$$y_W = 293.16 - 57.18dv_1 - 7.26dv_2 + 5.74dv_3$$
$$- 0.44dv_4 - 4.43dv_5 + 5.03dv_6 - 3.06dv_7 \quad (11)$$
$$+ 0.13dv_1^2 + 0.9dv_1dv_2 + 0.17dv_1dv_5 + 0.39dv_1dv_7$$

The adjusted coefficients of determination of the holding force, maximum thrust, action complete time, and P.M. weight are 99.9 [%], 99.2 [%], 95.1 [%], and 100 [%], respectively, and the response surfaces for each response function are expressed using (8)-(11), as shown in Fig. 12, which shows the contour lines and optimal points for each design variable.

In order to investigate the influence of significant parameters on the design results, the magnitude and importance of the impact of each design variable on the response functions is analyzed by means of the Pareto chart shown in Fig. 13. It can be seen that the design variable dv_7 is most significant for the holding force, maximum thrust, and action complete time. Because design variables such as dv_1, dv_2, and dv_7 represent the dimensions of the P.M., these three variables come to the effective design variables
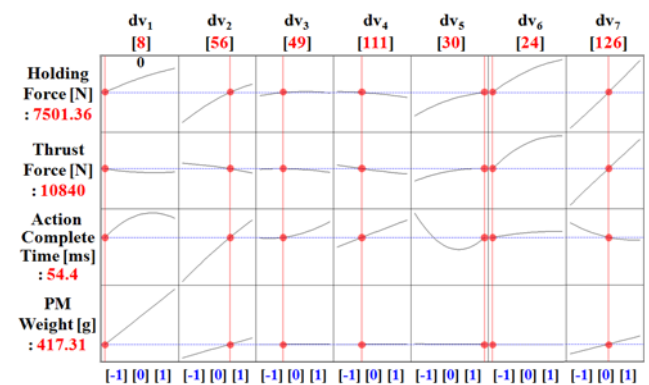

Fig. 12. Contour lines and optimal points around each response function
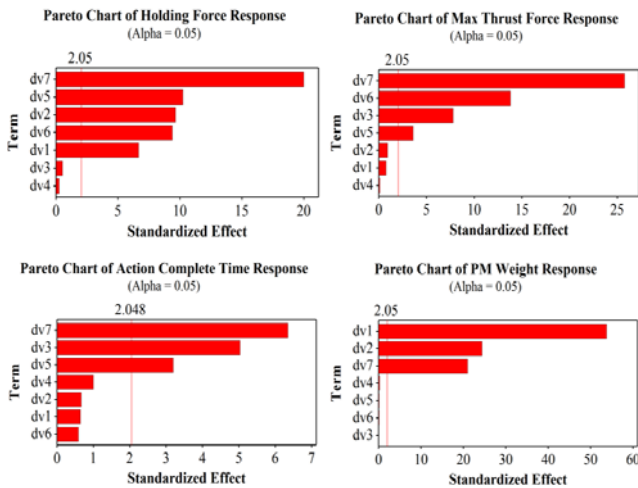
Hyun-Mo Ahn, Tae-Kyung Chung, Yeon-Ho Oh, Ki-Dong Song, Young-Il Kim, Heung-Ryeol Kho, Myeong-Seob Choi and Sung-Chin Hahn

Fig. 13. Pareto chart of the standardized effects for each response function.

Table 4. Optimal design results for P.M.A. model

Classification	DV_1	DV_2	DV_3	DV_4	DV_5	DV_6	DV_7
Optimal Value [mm]	8	56	49	111	30	24	126

Table 5. Comparison of initial model and optimal model

Classification	Initial Model (A)	Optimal Model		Comparison [%]	
		R.S.M. (B)	F.E.A. (C)	(B-C)/B	(A-C)/A
Holding force [N]	7777.2	7501.4	7397.5	1.4	-4.9
Max thrust force [N]	11173.2	10840	10842.5	-0.02	-3
Action complete time [ms]	54.8	54.4	54.2	0.4	-1.1
PM weight [g]	501.4	417.3	417.7	-0.1	-16.7

determining P.M. weight. The Pareto chart shows absolute value of the effects of each design variable. The optimal P.M.A. model obtained from R.S.M. is shown in Table 4.

Dynamic characteristics such as the holding force, maximum thrust, action complete time, and P.M. weight are compared between the initial and optimal models in Table 5.

As shown in Table 5, the action complete time has been shortened from 54.8 [ms] to 54.2 [ms], and the P.M. weight decreases by 16.7 [%]. Even though the action complete time of the P.M.A. becomes a little faster, we think that the performance of P.M.A. is improved by the proposed method.

6. Conclusion

In this paper, a design optimization process to minimize P.M. weight and to improve the dynamic characteristics of an initially designed P.M.A. model was proposed. In order to verify the validity of numerical analysis based on coupled F.E.M. used in this process, the dynamic characteristics of P.M.A. were compared with experimental results from no-load test and show good agreements.

In order to optimize the initial P.M.A. model, an optimal design process was performed by the proposed R.S.M. using the mixed orthogonal arrays table based on seven design variables and their three levels. In order to verify the validity of the proposed optimizing process, the optimal P.M.A. model was then compared with the initial P.M.A. model. As the optimal designed P.M.A. model shows improved performance relative to the initial model, we conclude that the proposed approach is efficient to improve the performance of the optimal designed P.M.A. and to reduce the number of experiments by the proposed R.S.M. using the mixed orthogonal array table. We therefore believe that this process will be useful in the design optimization of power apparatuses.

References

[1] D. D. Shipp, T. J. Dionise, V. Lorch, and B. G. MacFarlane, "Transformer Failure Due to Circuit-Breaker-Induced Switching Transients", *IEEE Trans. Ind. Appl.,* vol. 47, no. 2, pp. 707-718, Mar./Apr., 2011.

[2] D. D. Shipp, T. J. Dionise, V. Lorch, and W. G. MacFarlane, "Vacuum Circuit Breaker Transients During Switching of an LMF Transformer", *IEEE Trans. Ind. Appl.,* vol. 48, no. 1, pp. 37-44, Jan./Feb., 2012.

[3] A. Iturregi, E. Torres, I. Zamora, and O. Abarrategui, "High Voltage Circuit Breaker: SF6 vs. Vacuum", in Proc. *the 7nd Int. Conf. Renewable Energies and Power Quality 2009*, pp. 1-6.

[4] K. N. Park, J. W. Son, and S. C. Hahn, "Dynamic Characteristic Analysis of Permanent Magnetic Actuators Coupled Electromagnetic-mechanical Finite Element Method", in *Proc. 2010 International Conference on Electrical Machines and Systems*, pp. 1706-1709.

[5] S.Fang, H.Lin, and S.L. Ho, "Transient Co-Simulation of Low Voltage Circuit Breaker with Permanent Magnet Actuator", *IEEE Trans. Mag.*, vol. 45, no. 3, pp. 1242-1245, Mar., 2009.

[6] S. K. Hong, J. S. Ro, and H. K. Jung, "Optimal

Design of a Novel Permanent Magnetic Actuator using Evolutionary Strategy Algorithm and Kriging Meta-model", *J Electr. Eng. Technol.*, vol. 9, no. 2, pp. 471-477, Mar., 2014.

[7]   S. Fang, H. Lin, S. L. Ho, X. Wang, P. Jin, and H. Liu, "Characteristics Analysis and Simulation of Permanent Magnet Actuator with a New Control Method for Air Circuit Breaker", *IEEE Trans. Mag.*, vol. 45, no. 10, pp. 4566-4569, Oct., 2009.

[8]   J. R. Brauer, *Magnetic actuators and sensors*, Wiley-Interscience, 2006.

[9]   D. K. Hong, B. C. Woo, D. H. Koo, and D. H. Kang, "Optimum Design of Transverse Flux Linear Motor for Weight Reduction and Improvement Thrust Force Using Response Surface Methodology", *IEEE Trans. Mag.*, vol. 44, no. 11, pp. 4317-4320, Nov., 2008.

[10] A. Khuri and S. Mukhopadhyay, "Response Surface Methodology: Advanced Review", *WIREs Comp. Stat.*, vol. 2, no. 2, pp. 128-149, Mar./Apr., 2010.

[11] D. K. Hong, B. C. Woo, and C. W. Ahn, "Optimum Design for Improvement of PM-type Longitudinal Flux Linear Motor Using the Statistical Methods", *International Journal of Modern Physics B*, vol. 24, no. 15n16, pp. 2821-2826, Jun., 2010.

[12] A. M. Omekanda, "Robust Torque and Torque-per-inertia Optimization of a Switched Reluctance Motor using the Taguchi method", *IEEE Trans. Ind. Appl.*, vol. 42, no.2, pp. 473-478, Mar./Apr., 2006.

[13] D. K. Hong, B. C. Woo, D. H Koo, and K. C. Lee, "Electromagnet Weight Reduction in a Magnetic Levitation System for Contactless Delivery Applications", *Sensors*, vol. 10, no. 7, pp. 6718-6729, Jul., 2010.

[14] P. G. Slade, *The vacuum interrupter - theory, design, and application*, CRC Press, 2008.

[15] S.H. Khan, M. Cai, T.V. Grattan, K. Kajan, M. Honeywood, and S. Mills, "Computation of 3-D Magnetic Field Distribution in Long-Lifetime Electromagnetic Actuators", *IEEE Trans. Mag.*, vol. 43, no. 4, pp. 1161-1164, Apr., 2007.

[16] J. S. Ro, S. K. Hong, and H. K. Jung, "Characteristic Analysis and Design of a Novel Permanent Magnetic Actuator for a Vacuum Circuit Breaker", *Electric Power Applications, IET*, vol. 7, no. 2, pp. 87-96, Feb., 2013.

[17] G. E. P. Box, J. S. Hunter, and J. S. Hunter, *Statistics for Experimenters: Design Innovation, and Discovery*, Wiley-Interscience, 2005.

[18] H. M. Hasanien, A. S. Abd-Rabou, and S. M. Sakr, "Design Optimization of Transverse Flux Linear Motor for Weight Reduction and Performance Improvement Using Response Surface Methodology and Genetic Algorithms", *IEEE Trans. Energy Convers.*, vol. 25, no. 3, pp. 598-605, Sep., 2010.

[19] J. Xie, D. H. Kang, B. C. Woo, J. Y. Lee, Z. H. Sha, and S. D. Zhao, "Optimum Design of Transverse Flux Machine for High Contribution of Permanent Magnet to Torque Using Response Surface Methodology", *J Electr. Eng. Technol.*, vol. 7, no. 5, pp. 745-752, Sep., 2012.

Hyun-Mo Ahn He received the B.S. and M.S. degrees in electrical engineering from Dong-A University, Busan, Korea, in 2009 and 2011, respectively. He is currently working toward the Ph.D. degree. His research interests are multi-physics analysis and numerical analysis of power apparatus and electric machines.

Tae-Kyung Chung He received the B.S., M.S., and Ph.D. degrees in electrical engineering from Seoul National University in 1981, 1983, and 1987, respectively. From 1986 to 1987, he worked at Daewoo Heavy Industries as a senior researcher. Since 1988, he has been with the School of Electrical and Electronics Engineering at Chung-Ang University in Korea as a professor. In 1991, he was with Harvey Mudd College in California as a visiting scholar. His main research fields are design of electric motors and actuators.
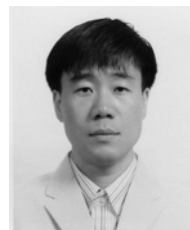
Yeon-Ho Oh He received the B.S. and M.S. degrees in electrical engineering from Dong-A University, Busan, Korea, in 1991 and 1993, respectively. He is currently a Research Engineer with the Power Apparatus Research Center, HVDC Research Division, Korea Electrotechnology Research Institute (KERI). He is now Team Leader for the estimation of the power apparatus with numerical analysis.

Ki-Dong Song He received the B.S. and M.S. degrees in electrical engineering from InHa University, Incheon, Korea, in 1988 and 1990, respectively. He got his Ph.D. degree in electrical engineering from Busan National University in 2003. He is currently a Research Engineer with the Power Apparatus Research Center, HVDC Research Division, Korea Electrotechnology Research Institute (KERI). His research interests focus on analysis and design for AC Power Devices and HVDC circuit breakers.

Young-Il Kim He received the B.S. degrees in mechanical engineering from Korea Aerospace University, Goyang, Korea, in 1990. He is currently an Executive Director of Power Apparatus R & D Institute in ENTEC Electric & Electronic Co., Ltd.

Heung-Ryeol Koh He received the B.S. degrees in electrical engineering from Hanyang University, Seoul, Korea, in 1990. He is currently a Senior Researcher of Power Apparatus R & D Institute in ENTEC Electric & Electronic Co., Ltd.

Myeong-Seob Choi He received the B.S. degrees in physics and M.S. degrees in electrical engineering from Soonchunhyang University, Asan, Korea, in 2002 and 2004, respectively. He is currently a Senior Researcher of Power Apparatus R & D Institute in ENTEC Electric & Electronic Co., Ltd.

Sung-Chin Hahn He received the B.S., M.S., and Ph.D. degrees in electrical engineering from Seoul National University, Seoul, Korea. He is currently a Professor with the Department of Electrical Engineering, Dong-A University, Busan, Korea, and senior member of the Korean Institute of Electrical Engineers (KIEE). His current research covers multi-physics analysis and design of power apparatus and electric machines.